



ELSEVIER

Contents lists available at ScienceDirect

## Computer Communications

journal homepage: [www.elsevier.com/locate/comcom](http://www.elsevier.com/locate/comcom)

# Virtual Network Embedding for telco-grade network protection and service availability

Ashiq Khan<sup>a</sup>, Xueli An<sup>b,1,\*</sup>, Shigeru Iwashina<sup>a</sup>

<sup>a</sup>Research Laboratories, NTT DOCOMO, Inc., Tokyo, Japan

<sup>b</sup>DOCOMO Communications Labs Europe GmbH, Munich, Germany

## ARTICLE INFO

## Article history:

Received 3 January 2015

Revised 18 February 2016

Accepted 14 March 2016

Available online xxx

## Keywords:

Virtual Network Embedding

Network virtualization

Network protection

Telecom networks

## ABSTRACT

The decoupling of software from hardware by means of virtualization presents us with a unique opportunity to perform on-the-fly network deployment and reconfiguration. Virtual Machines could be instantiated and virtual links can connect these machines to form end-to-end virtualized networks on top of a physical network infrastructure. Virtual Network Embedding (VNE) algorithms could be used to map such virtual network on a physical network infrastructure. However, present VNE algorithms do not consider overall network protection. This is critical for a Telecom operator that needs to realize 99.999% network availability. Moreover, VNE is an NP-hard problem. In this paper, we propose a heuristics VNE aimed at protecting Telecom operator sites. Our objective is to develop advance counter-measures in the form of telco-grade redundancy to avoid large scale network failures such as the one observed during the tsunami in Japan in 2011. In designing our VNE algorithm, we distinguish server nodes from switching nodes as a server function cannot be embedded on a switching node. We also choose not to employ path splitting which is difficult to implement in real network operations. Along with detail modeling of our proposal, we also evaluate our scheme which shows its efficiency in realizing operators' valuable infrastructure protection while maintaining lower resource consumption.

© 2016 Published by Elsevier B.V.

## 1. Introduction

Network virtualization has gained large momentum in the research community over the recent years and is now moving towards commercialization. Extensive usage of network virtualization can be observed in the datacenters or clouds in the IT sector where service availability and the consequent protection requirements are not so stringent. Telecom operators are also becoming increasingly interested in network virtualization. Some potential use cases in the Telecom sector [1] are the ease of deployment of nodes like MME, S/P-GW [2], on-demand scaling of such nodes based on instant load rather than peak load based over-provisioning [3], dynamic topology reconfiguration for disaster avoidance and recovery [4], etc.

Network virtualization consists of computing node virtualization and communication link/path virtualization. This creates virtualized end-to-end networks on a Physical Network Infrastructure (PNI). Virtual Machine (VM) virtualizes computing nodes or

network functions. For transport network virtualization, Software-Defined Networking (SDN) has become a prominent candidate for virtualizing communication links/paths. The key features of virtualization are isolation among virtualized entities i.e. VMs and Virtualized Links (VLs), and decoupling of software from hardware. Isolation among virtualized entities enables the coexistence of multiple Virtualized Networks (VNs) in the same PNI e.g. different generations of cellular networks [5]. The independence of software e.g. VM from the underlying hardware enables on-the-fly network creation, which takes years at present in physical network deployments. The PNI is a static entity on top of which, VNs with different topologies, computing and link resources can be created, operated and removed on demand. This enables faster network deployment, reduces occupying resources when not necessary, and thus improves resource usage efficiency of a PNI to maximize revenue. Such decoupling between software and hardware also enable VMs and VLs migration [6]. Such characteristics can be used to migrate critical network facilities, when virtualized, to safer location during natural disasters.

Such automated and on-demand VN generation can be performed by Virtual Network Embedding (VNE) techniques. A VNE request consists of a VN topology, necessary computing and link resources e.g. number of VMs per computing node in the requested topology, link Bandwidth (BW), delay and other requirements. A

\* Corresponding author. Tel.: +49 1781320572.

E-mail addresses: [khan@nttdocomo.com](mailto:khan@nttdocomo.com) (A. Khan), [an\\_de\\_luca@docomolab-uro.com](mailto:an_de_luca@docomolab-uro.com), [anxueli@gmail.com](mailto:anxueli@gmail.com) (X. An), [iwashina@nttdocomo.com](mailto:iwashina@nttdocomo.com) (S. Iwashina).

<sup>1</sup> Present address: European Research Center, Huawei Technologies, Munich, Germany.

VNE algorithm then finds out the best possible mapping i.e. embedding solution of such requests on a PNI. VNE is an NP-hard problem [7]. Many heuristics have been proposed with a view to finding a workable polynomial time solution. A major drawback is that network protection aspects are largely absent in the existing solutions. Many schemes are available for path protection in the form of multi-path redundancy. However, site e.g. datacenter protection schemes are not available. Network paths are stateless and if paths are lost, service does become unavailable. However, it does not destroy user or operational data. If a site is destroyed, uncountable amount of user and network operation data are lost. In this paper, a site refers to a datacenter or cloud, consisting of a collection of physical servers. Sites are assumed to be geographically distributed i.e. a Telecom operator or a service provider has multiple such sites in a country, connected by a core transport network. In this paper, we consider such sites hosting telecom node functions [2] in the form of VMs, which require high service availability. For modeling purposes, a site is sometimes referred to as a site node which is an abstraction of the whole site to a single network node providing computational and storage resources.

In this paper, we propose a polynomial time VNE algorithm for telecom operators site protection. Our objective is to design a solution which can provide protection for all sites in an operators network [8]. There is no less critical site for an operator, who is bound by regulatory constraint on service availability of 99.999% (five 9s). This results in a downtime of around 5 min a year [9]. The conventional 1 + 1 protection scheme employed by the Telecom operators is based on such a constraint. Unlike the available site protection schemes which address a single-site failure at a time, our objective is to provide solution for simultaneous multiple-site failures. Therefore, our aim is to develop a VNE algorithm which provides a 1 + 1 redundancy to all Telecom sites so that any number of site failures can be recovered without service interruption. This comes from our experience with the earthquake/tsunami in March 2011 in Japan, where Telecom operators experienced large-scale network failures over a prolonged period of time. We explicitly do not address path protection in this paper because of the availability of in-depth research in this area which has resulted in a number of path protection schemes [18–22]. We do address link embedding in this paper to the extent of the correlation between link embedding and node embedding to improve the overall VNE performance. Correlation between node embedding and link embedding is largely absent in existing VNE methods, where a two-step approach is adopted – first, selection of the nodes, then discovery of paths among the selected nodes to embed the requested links. In such approaches, a node having sufficient computational resources but not sufficient link resources can be selected as potential candidate to embed a virtual node. Such nodes are discarded in the second step where the link embedding algorithm discards such nodes with insufficient bandwidth. To avoid this inefficiency, we only select those nodes that have sufficient ingress/egress link bandwidth to host the consequent VNs. This correlation between node and link embedding is also an originality of our proposal.

The scope of this paper is to propose a polynomial time heuristic VNE for Telecom site protection, where a backup site is explicitly found for each site in a VNE request. Our objective is to put forward an efficient VNE which achieves the above but with higher resource usage efficiency compared to existing solutions. We restrict ourselves to the theoretical evaluation of the VNE algorithm itself in terms of its success rate, and how much network resources the VNE solution consumes. In this paper, we do not address the site recovery procedure i.e. exactly when and how a primary site is switched over to a backup site. Such decision depends on telecom operators operational principles, as well as the particular node backup mechanism involved (e.g. hot standby). In this paper, our objective is to ensure that a backup site is found which realizes a

telco-grade 1 + 1 protection scheme for all Telecom sites. The consequent evaluation of switching mechanism to backup sites during failures is an important item to further evaluate the efficiency of our proposed solution in practical network operations, and we intend to address this in our future work.

The rest of the paper is organized as follows: Section 2 discusses related work. Section 3 presents our network model and formulates the VNE problem mathematically. In Section 4, we present our site-protection VNE algorithm, and provide evaluation results in Section 5. In Section 6 we discuss how to use such VNE algorithms in a Network Functions Virtualization (NFV) context. Section 7 concludes the paper with a summary and areas for future exploration.

## 2. Related work

ViNEYard [7] proposes VNE algorithms where node mapping is coordinated with link mapping. Here, VNE is formulated as Mixed Integer Linear Program (MIP). As MIP is computationally intractable, they relax the integer constraints to obtain a Linear Program (LP) which can be solved in polynomial time. However, they use location as a requesting parameter in a VNE request. This limits the embedding location of a VNE request. It potentially overloads a certain locality of a physical network infrastructure whereas other parts of the infrastructure may remain underutilized. They also use Multi-Commodity Flow (MCF) which embeds a virtual link over multiple physical paths by path splitting, thus increasing the success rate of a VNE. However, path splitting is not supported in real commercial public network. Routers do not keep multiple paths to a certain destination and even if they do, they do not use them simultaneously for the same session. Besides, sending packets of the same session over multiple paths leads to packet reordering problem in the end host, as different packets arrives in a different order due to different lengths of the paths. Packets out of sequence are usually discarded.

Authors in [10] propose two Fault-Tolerant VN Embedding (FTE) approaches. These are FTE-PP for protection in the physical layer and, FTELP for protection in the logical or VN layer. The FTE-PP provides two protection paths for each link, and focuses on minimizing the backup resources necessary for such redundancy. FTELP augments a VN topology with redundant resources so that a VN survives physical link/node failure by using the redundant resources. In our proposal, we provide 1 + 1 backup for a site. However, it does not necessarily mean that the backup sites cannot be used for other purposes in the absence of a failure in the primary site e.g., allocating to low priority services. In [10], the authors assume that the substrate network (PIP) is not operational all the time. The authors re-emphasize our statement that although there are numerous physical link protection schemes available, little work has been done on node failure protection.

However, in this work, the node mapping and the link mapping remains uncorrelated which, as demonstrated by the authors in [7], leads to suboptimal VNEs as well as extra complexity for the embedding process itself. The most significant difference between the research presented in [10] and our solution is that the authors in [10], like most other related work, assume that there are no simultaneous multiple node or link failures. Our solution is entirely based on the assumption that there are indeed cases where simultaneously multiple nodes/sites fail, e.g. during large scale natural disasters. The proposal in [10] solely focuses on protection against single-node or link failure.

Authors in [11] propose a heuristic Virtual Network Embedding techniques that increase the survivability of the embedded virtual network by means of node migration and link remapping. They use the Artificial bee colony algorithm to achieve optimal Virtual Network Embedding. When a node fails (a node is a site in the

context of our proposal), it is migrated to a normal node. After that, affected links are all remapped by using the shortest path algorithm. However, as mentioned before, a mobile Telecom network which is the primary focus of this work, has a service availability requirement of five 9s. Searching for a new node after the failure and then migrating a heavy telco node virtual machine requires significant time [12]. To meet telecom service availability requirements that are also regulatory, we not only prepare a backup node beforehand, but also prepare it at a reasonable network distance so that switching over to the backup node once the primary node fails could be done within Telecom service availability requirements. For voice service, fail-over needs to be performed in less than a second.

Authors in [13] propose a reliability-aware heuristic VN embedding algorithm, where they try to minimize the over-provisioning of network resources necessary for such reliability, in other word, redundancy. They assume a heterogeneous failure rate for different elements in the Physical Network Infrastructure (PNI), which, we believe, is a realistic assumption. They then calculate the overall reliability based on the heterogeneity of the PNI elements. In their model, a VNE request comes with its reliability requirement which needs to be met during the VNE process. However, as the authors themselves point out, measuring the reliability of a VN is a daunting task. To reduce the problem space, they define protection-domains where, failure of one element in the domains leads to the failure of the whole domain. Such clustering reduces the number of elements needed to be considered in order to measure the overall reliability of a VN. However, while performing the VNE taking the overall required reliability of a requested VN, this proposal uses Multi-Commodity Flow (MCF), which we consider unrealistic in real network operation (see Section 1).

Authors in [14] consider regional disasters to be of stochastic nature and incorporate this when they perform VNE for improved reliability. They estimate risk values for different regions and consequently perform the VNE with such risk-awareness. We consider this work very suitable to disaster-prone regions like Japan where strong earthquakes are frequent. As explained in detail in Section 4.1, our backup site mapping considers a network distance from the primary site to its backup site so that both do not fail simultaneously. The proposal in [14] could be an efficient way to define such network distance so that the primary and backup sites are not mapped in the same failure region e.g. continental plates. However, we generalize this aspect rather than explicitly focus on disaster-prone regions so that our scheme could be used in any arbitrary site failure scenario.

Authors in [15] address the topic of this paper i.e. survivable VN design by means of protection against site node ('facility node' in their term) failure. They propose two heuristic schemes which extend the target VN for redundancy during embedding, and then improve resource usage efficiency by enabling resource sharing between primary and backup sites. The Extended Virtual Network (EVN) approach before embedding taken in [15] is similar to our approach where we extend the requested VN first for our objective of simultaneous multiple site failure protection. However, this work purely focuses on recovery from a single site node failure and proposes a resource efficient way to design an  $N+1$  VN topology ( $N$  is the number of site nodes in the original VNE request). The proposed scheme in [15] will fail to provide protection during simultaneous multiple site failures, which is the main focus of our work.

Authors in [16] assume a flexible optical grid transport plane which is controlled by a Software Defined Network (SDN) controller. The controller takes a VNE decision, and performs the embedding to realize link protection and node ('site' in our context) protection. However, they consider a shared protection scheme which reduces resource consumption necessary for redundancy at

the expense of the number of failures the system could recover from. From the node perspective, a node, which has sufficient resources to backup all other nodes, is selected as the shared backup. Creating such resource-heavy single site in a Telecom network is a formidable task. Further, the authors in [16] consider a particular transport network topology i.e. optical grid, whereas we do not restrict ourselves to any particular topology. Our network model is sufficiently robust to accommodate any present, as well as future network topology that could appear due to the flexibility provided by network virtualization.

Authors in [17] present a heuristic VNE algorithm which takes into account the substrate node reliability awareness during the embedding process. In their proposal, they first rank the substrate network nodes based on their reliability and resource load. They then chose the high ranking nodes to optimize reliability against resource consumption. However, the focus remains on minimization of node resource consumption rather than redundancy for failure recovery. The proposed scheme relies on the high reliability value of a chosen substrate node. In real-life network operation, all nodes fail—highly reliable or not. Besides, highly reliable nodes cannot avoid failure in natural disasters which is our focus area for improved protection and reliability.

Including the works presented above, most network protection and service availability schemes aim at optimizing network redundancy against resource consumption. This leads to an  $N+K$  protection scheme where  $N>K$ . Here,  $N$  is the number of site nodes in the requested VN, and  $K$  is number of backup sites for  $N$  site nodes. Our proposal is an explicitly  $N+N$  protection scheme which is a telco service requirement. And, an  $N+N$  protection scheme can always be reduced to an  $N+K$  protection scheme without any added complexity, but not vice versa. Extending an  $N+K$  protection scheme to an  $N+N$  protection scheme is not straightforward. If executed along the lines of the conventional approach described in Section 4, it becomes very inefficient from the point of view of resource consumption, as would be shown in Section 5 of this paper. The motivation to develop a robust  $N+N$  protection scheme is further underlined by this issue.

In the existing literature, link protection schemes have been exhaustively investigated. Our focus in this paper is not on link protection; rather, the protection of high-availability Telco-sites, which hold data of millions of customers per-site. Existing link-protection schemes [18–20] can be readily used with our scheme to realize link protection. However, in relation to multiple simultaneous link failures, we present two recent works which can become useful under such failure scenarios.

Authors in [21] confirm our finding that a live migration-based protection scheme would not suffice to limit the service downtime to below a reasonable value [9]. They propose Opportunistic Resilience Embedding (ORE) which proactively maps a virtual link to multiple physical paths for protection reasons. They also have a reactive step which tries to recover the lost capacity after a failure. Although we do not explicitly address link protection, but rather try to minimize link resource consumption during a VNE process, mapping a virtual link to multiple substrate paths will consume substantially more link resources than in our scheme. However, as the path redundancy level is quite high, ORE [18] can be a suitable technique to recover from multiple simultaneous link failures. In our view, this proposal can fit very well with ours where we ensure simultaneous multiple site failures, whereas this scheme is used to recover from simultaneous multiple link failures, both of which are observed during large scale natural disasters.

The work presented in [22] provides a modeling scheme for VNE, where the link availability constraints are added to the links in a VNE request. As VNE is an NP-hard problem, authors in [22] present a heuristic which meets the link availability requirement in a VNE request. The heuristic selects multiple physical

**Table 1**  
Summary of related work.

Related work	Features					
	Link-node correlated embedding	No path splitting	Server-switch distinction	Limited site protection	All site protection	Proactive approach
ViNEYard [7]	Yes	No	No	No	No	Yes
FTE [10]	No	Yes	Partially	Yes	No	Yes
Migration-based [11]	No	Yes	No	Yes	No	No
Reliability aware [13]	No	No	No	Yes	No	Yes
Region failure [14]	Yes	Yes	No	Yes	No	Yes
Survivable VN [15]	Yes	No	No	Yes	No	Yes
Optical grid [16]	No	Yes	No	Yes	No	Yes
Selected protection [17]	No	Yes	No	Yes	No	Yes
Our proposal	Yes	Yes	Yes	Yes	Yes	Yes

Q3

304 paths, where the total availability over all the selected physical  
 305 paths can meet the requested availability of one VL. Thus, one VL,  
 306 depending on the physical links it is being mapped on, can have  
 307 multiple backup paths. This is a realistic approach in ensuring link  
 308 failure recovery as the conventional 1 + 1 link protection may not  
 309 suffice if the underlying physical links availability values are too  
 310 low.

311 In Table 1, we present a summary of the related body of work  
 312 focusing on the research that explicitly mentions site protection.  
 313 In our view, the link protection schemes can be used with most  
 314 site protection schemes. Table 1 clearly positions our proposal and  
 315 shows its scope compared to other relevant work. The higher num-  
 316 bers of ‘Yes’ shows the proximity to our work in this paper. Proac-  
 317 tive approach refers to the case where a protection scheme is de-  
 318 termined and deployed beforehand. Table 1 should be viewed in  
 319 conjunction with the detailed comparison provided above.

### 320 3. Modeling and problem formulation

321 In future commercial networks, a VNE request will come from  
 322 a Virtual Network Operator (VNO) which wishes to provide ser-  
 323 vice using the PNI. Fig. 1a shows an operational structure [5] of  
 324 the process. Operators Network Operation System will receive such  
 325 VNE requests, and embed them in the PNI. The PNI consists of two  
 326 components: the sites and the core transport network. A site here  
 327 is a datacenter/cloud (shown as a cloud in Fig. 1a), consisting of  
 328 numerous physical server machines. These sites are geographically  
 329 distributed over a large area e.g. a country, and the core trans-  
 330 port network provides connectivity among these sites. We envi-  
 331 sion that the sites with computation and storage capabilities can  
 332 be used to host services like 3GPP core network nodes/functions,  
 333 e.g. MME, S/P-GW, etc., which can be deployed in the form of VMs  
 334 on physical machines. Such mobile core nodes are conventionally  
 335 deployed in a geographically distributed way to perform mobility  
 336 management and user plane aggregation closer to mobile users.  
 337 Upon a particular VN embedding request, these mobile core net-  
 338 work nodes are embedded in the PNI. The graphical interpretation  
 339 of the scenario explained above is shown in Fig. 1b. The Telecom  
 340 sites in Fig. 1a are modeled as single-site nodes in Fig. 1 b. The  
 341 numbers shown in Fig. 1b beside these represent their capacity,  
 342 such as the number of VMs this site can accommodate at the mo-  
 343 ment, or the number of physical machines available etc. The core  
 344 transport network consists of switching nodes and links connect-  
 345 ing the site nodes. Links can be specified by their BW limitation  
 346 and delay ( $d$ ) values.

#### 347 3.1. Network model

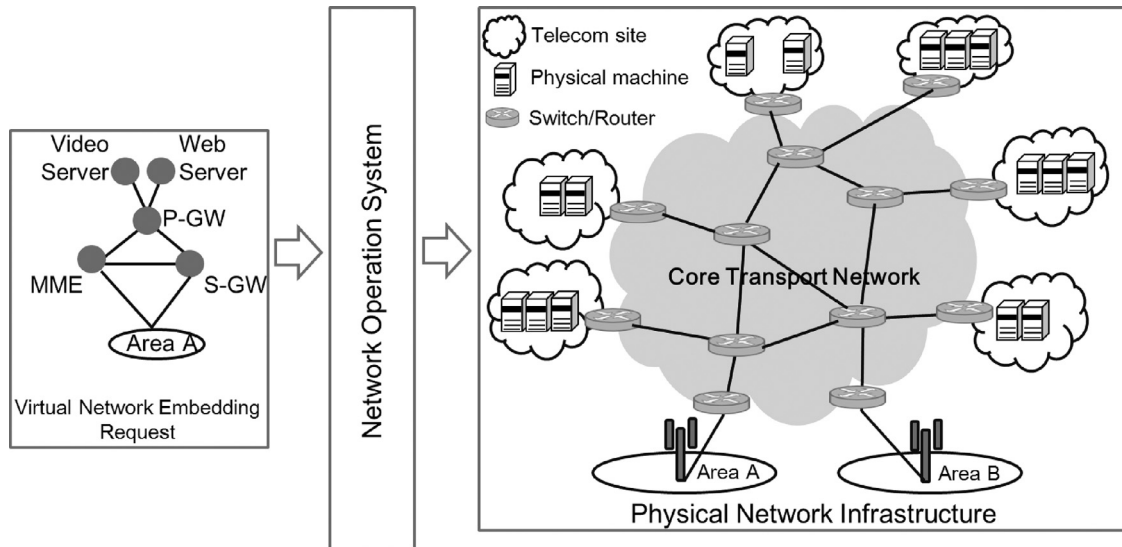
348 The entire PNI can be modeled as a graph  $G_p = (V_p, E_p)$ , where  
 349  $V_p$  and  $E_p$  represent the set of vertices/nodes and the set of links  
 350 within the PNI, respectively. We use  $|V_p|$  to denote the number of

351 nodes in the set of  $V_p$ . We use  $n_p^i$  to refer to a node with ID  $i$  which  
 352 belongs to set  $V_p$ ,  $\forall n_p^i \in V_p$ . A link between node  $i$  and  $j$  is given by  
 353  $e_p(i, j)$ , and  $\forall e_p \in E_p$ . The adjacency matrix of  $G_p$  is given by  $A_p$ ,  
 354 which is a  $|V_p| \times |V_p|$  matrix. If there is an incident link between  
 355 node  $i$  and  $j$ ,  $A_p(i, j) = 1$ ; otherwise,  $A_p(i, j) = 0$ . A bidirectional  
 356 graph is assumed in this work, hence  $A_p(i, j) = A_p(j, i)$ . A path  
 357 from source node  $i$  and destination node  $j$  is denoted as  $p(i \rightarrow j)$ ,  
 358 which is the collection of the links along the path. The path length  
 359 is given by  $|p(i \rightarrow j)|$ .  $\vec{i}$  and  $\vec{j}$  represent a set of sources and desti-  
 360 nations, hence  $p(\vec{i} \rightarrow \vec{j})$  is the set of paths containing all the com-  
 361 binations of the sources and destinations.  $P_p$  represents the set of  
 362 all the feasible paths within  $G_p$ . Therefore, if the source and desti-  
 363 nation are physical nodes ( $\forall n_p^i, n_p^j \in V_p$ ), then the notation  $p(i \rightarrow j)$   
 364 represents a physical path, which can be represented as  $p(i \rightarrow j) \in$   
 365  $P_p$ . The set of switching nodes within the core transport network  
 366 is given by  $V_s$  and the set of site nodes are represented as  $V_r$ ,  
 367 hence we have  $V_p = V_s \cup V_r$  on condition that  $V_s \cap V_r = \phi$ . Node ca-  
 368 pacity is specified by a  $a \times |V_p|$  array  $C_p$ , in which, the capacity of  
 369 node  $i$  is  $C_p(i)$ . The link BW is specified by a  $|V_p| \times |V_p|$  matrix  $B_p$ .  
 370 For a link  $e_p(i, j) \in E_p$ , its available BW is given by  $B_p(i, j)$ . The  
 371 available BW on a path  $p(i \rightarrow j)$  is denoted by  $f_p^{i \rightarrow j}$ , the value of  
 372 which is limited by the intermediate link that has the minimum  
 373 BW as  $f_p^{i \rightarrow j} = \min(B_p(i, v_1), \dots, B_p(v_{|p(i \rightarrow j)|-1}, j))$ , where  $v_i$  for  $\forall i \in$   
 374  $[1, |p(i \rightarrow j)| - 1]$ , is an intermediate node on the path.

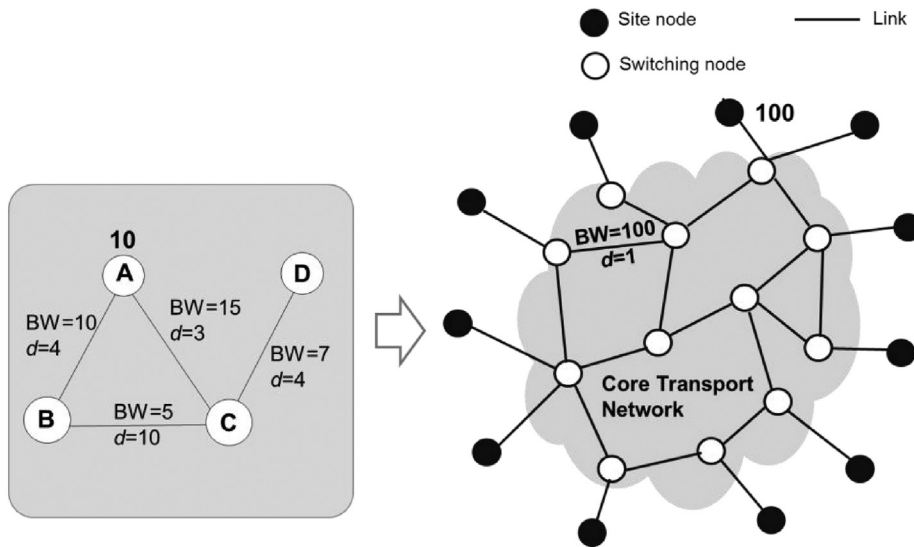
#### 375 3.2. Virtual Network Embedding request

376 The VNE request can come in different granularities. If a VNO  
 377 chooses to operate its virtual network at router level and above, it  
 378 can send a request in that detail. As this work is about site pro-  
 379 tection, we assume that a VNO sends its embedding request at site  
 380 granularity. A VNE request consists of VN nodes and links, which  
 381 can also be represented by an undirected graph  $G_v = (V_v, E_v)$  with  
 382 adjacency matrix  $A_v$ . Beside the VN topology, the VNE request also  
 383 provides the requirement constraints in terms of node capacity  $C_v$ ,  
 384 link BW  $B_v$  and delay limits  $D_v$ . Delay can be defined by round trip  
 385 time (RTT) or hop count. We assume that the dominant factor of  
 386 delay is the processing time when packets pass through a switch-  
 387 ing node, hence we use hop count as a parameter to model delay.  
 388 Fig. 1b provides an example of a VNE request, which consists of  
 389 four nodes with capacity, link BW, and delay requirements. Once  
 390 a VNE request arrives, it will be mapped to the PNI, which means  
 391 that a number of site nodes will be selected within the PNI, and  
 392 the bandwidth among the site nodes will be reserved for hosting  
 393 service and communication purposes.

394 To host Telecom services like 3GPP core network nodes in VNs,  
 395 carrier-grade availability is compulsory. The embedded VNs should  
 396 be survivable and recoverable from any number of simultaneous  
 397 site failures. Providing 1 + 1 backup for all the sites is one solu-  
 398 tion to achieve this required high availability. Therefore, along with



a. Network operation for VNE



b. Graphical representation of VNE

Fig. 1. VNE request embedding.

399 one primary site, one backup site is also needed for mapping a VN  
 400 node. The backup site can be hot-standby and the running service  
 401 states are synchronized between the primary and backup sites at  
 402 all times, hence the backup site can take over the service immedi-  
 403 ately without interruption when the primary site goes down. How-  
 404 ever, the backup mechanism is out of the scope of this work. In  
 405 this paper, we focus on how to select and inter-connect the backup  
 406 and primary sites.

407 3.3. Problem formulation

408 The VNE problem can be considered as a process with two  
 409 stages: VN node mapping and VN link mapping. In the first stage,  
 410 VN nodes are mapped to site nodes in the PNI using function  
 411  $M_n : V_v \mapsto V_r$ . In order to achieve 1 + 1 site protection for VN node $i$ ,  
 412 a primary site node  $n_v^{i_p}$  and a backup site node  $n_v^{i_b}$  are selected to-

gether for VN node mapping:

$$\mathfrak{M}_n(n_v^i) = \{n_r^{i_p}, n_r^{i_b}\}, \quad \forall n_v^i \in V_v, \quad \forall n_r^{i_p}, n_r^{i_b} \in V_r, \quad n_r^{i_p} \neq n_r^{i_b} \quad (1)$$

In the second stage, the feasible paths between all the mapped  
 414 site nodes are established by using function  $M_l : E_v \rightarrow P_p$ , where,  
 415  
 416

$$\mathfrak{M}_l(e_v(i, j)) = p(\mathfrak{M}_n(n_v^i) \mapsto \mathfrak{M}_n(n_v^j)), \quad \forall n_v^i, n_v^j \in V_v \quad (2)$$

To guarantee the seamless service migration in the site failure  
 417 scenario, for instance for a VNE request with two nodes and one  
 418 link as shown in Fig. 2a, we have to explicitly search for two pri-  
 419 mary and two backup nodes, and six links between all the primary  
 420 and backup nodes to enable 1 + 1 site protection as illustrated in  
 421 Fig. 2b. This would be the conventional method to handle 1 + 1 site  
 422 protection. Hence, the total required BW to embed one VN link is  
 423 the summation of the reserved BW on all six links. The required  
 424

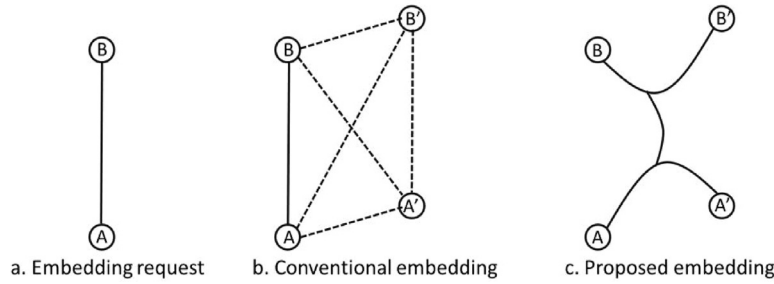


Fig. 2. 1 + 1 site protection illustration.

425 backup BW for the path between the primary and backup nodes  
 426 might be fewer than the requested BW on the primary path, which  
 427 depends on the selected backup mechanism as we mentioned be-  
 428 fore, or the explicit request from the VNO. For analysis simplicity,  
 429 we assume that the required backup BW is the same as the re-  
 430 quested BW for the primary path.  $\mathfrak{M}_l(e_v(i, j))$  defined in (2) is a  
 431 path set with two kinds of paths: data communication path set  
 432  $\mathfrak{M}_l^c(e_v(i, j))$  and backup path set  $\mathfrak{M}_l^b(e_v(i, j))$  where  $\mathfrak{M}_l^c(e_v(i, j)) =$   
 433  $\{p(i_p \rightarrow j_p), p(i_b \rightarrow j_b), p(i_p \rightarrow j_b), p(i_b \rightarrow j_p)\}$  and  $\mathfrak{M}_l^b(e_v(i, j)) =$   
 434  $\{p(i_p \rightarrow i_b), p(j_p \rightarrow j_b)\}$ . The VNE request embedding issue can be  
 435 formulated as an optimization problem as following:  
 436

Objective:

$$\min \sum_{e_v(i, j) \in E_v} B_v(i, j) \left( \sum_{p(x \rightarrow y) \in \mathfrak{M}_l^c(e_v(i, j))} |p(x \rightarrow y)| + \sum_{p(x \rightarrow y) \in \mathfrak{M}_l^b(e_v(i, j))} |p(x \rightarrow y)| \right) \quad (3)$$

Resource constraints:

$$C_v(i) \leq \min(C_r(i_p), C_r(i_b)), \forall n_r^i, n_r^j \in V_r \quad (4)$$

$$f_p^{i_p \rightarrow j_b} \geq \sum_{j=1, j \neq i}^{|V_v|} B_v(i, j), \forall n_v^i, n_v^j \in V_v \quad (5)$$

$$f_p^{x \rightarrow y} \geq B_v(i, j), p(x \rightarrow y) \in \mathfrak{M}_l^c(e_v(i, j)) \quad (6)$$

$$|p(x \rightarrow y)| \leq D_v(i, j), p(x \rightarrow y) \in \mathfrak{M}_l^c(e_v(i, j)) \quad (7)$$

$$\sum_{e_v(i, j) \in E_v} \left( \sum_{p(x \rightarrow y) \in \mathfrak{M}_l^c(e_v(i, j))} B_v(i, j) 1_{p(x \rightarrow y)}(e_p(u, v)) + \sum_{p(x \rightarrow y) \in \mathfrak{M}_l^b(e_v(i, j))} \sum_{j=1, j \neq i}^{V_v} B_v(i, j) 1_{p(x \rightarrow y)}(e_p(u, v)) \right) \leq B_p(u, v) \quad (8)$$

Node and link constraints:

$$x_{i, j} \in \{0, 1\}, \forall n_v^i \in V_v, \forall n_v^j \in V_r \quad (9)$$

$$x_{i, i_p} = 1, x_{i, i_b} = 1, \sum_{j=1, j \neq i}^{|V_v|} x_{j, i_p} = 0 \quad \text{and} \quad \sum_{j=1, j \neq i}^{|V_v|} x_{j, i_b} = 0 \quad (10)$$

$$x_{uv} \in \{0, 1\}, \forall n_p^u, n_p^v \in V_p, \forall e_p(u, v) \in E_p \quad (11)$$

$$\sum_{i: e_p(i, k) \in E_p} x_{ik} - \sum_{j: e_p(k, j) \in E_p} x_{kj} = \begin{cases} -1, & k = s, n_s^s \in V_r \\ 1, & k = d, n_r^d \in V_r, p(s \rightarrow d) \in P_p \\ 0, & n_s^k \in V_s \end{cases} \quad (12)$$

Eq. (4) represents the capacity constraint from a VNE request, which means that the selected primary and backup site nodes should have sufficient capacity to host it. Eq. (5) is the BW constraint for the path between the primary and backup site nodes, which are mapped from VNE node  $i$ . It implies that the reserved BW for this path is the summation of all the incoming and outgoing traffic from VN node  $i$ . Eqs. (6) and (7) are the BW and delay constraints for the communication paths. Eq. (8) implies that the total BW of all the flows passing through the physical link  $u \rightarrow v$  is limited by its available BW  $B_p(u, v)$ , in which  $1_A(a)$  is an indicator function and  $1_A(a) = 1$  if  $a \in A$ , otherwise,  $1_A(a) = 0$ .

In Eq. (9),  $x_{i, j}$  is a binary variable, which is 1 if site node  $j$  is selected as a primary or a backup node for VN node  $i$ . Otherwise, it is zero. Eq. (10) ensures that one site node can only accommodate one VN node (primary or backup) for one VNE request.  $\tilde{x}_{uv}$  introduced in Eq. (11) is also a binary variable which is equal to the indicator function  $1_{p(x \rightarrow y)}(e_p(u, v))$  defined in Eq. (8). Eq. (12) limits that, for all the intermediate switching nodes on the path  $p(s \rightarrow d)$ , the number of incoming links is equal to the number of outgoing links.

#### 4. Our proposal: VNE for telco site protection

As mentioned in the previous section, we aim to realize the telco-grade 1 + 1 protection scheme for all Telecom sites. 1 + 1 site protection is expensive in terms of bandwidth because the required bandwidth is not only reserved from the primary to primary sites, but also the path between primary to backup, and backup to backup sites. This is implemented in order to handle any number of primary site failures. Therefore, our main objective is to reduce the bandwidth consumption to embed the VNE requests.

At first, we select potential candidate site nodes in the PNI with enough resources to accommodate the requested nodes. In the second step, we form primary-backup site node pairs based on a predefined network distance between them. Once such candidate pairs for each VN node have been selected, the problem space is significantly reduced. Then, we embed the links among the pairs which satisfy both the BW and delay requirements from the VNE request. Multiple candidate pairs provide the flexibility to find out viable paths and optimize BW consumption.

## 485 4.1. Primary-backup pair searching

486 We consider all computing and storage resources (physi-  
487 cal/virtual machines) connected to the same access router as one  
488 logical site node. Therefore, we model the PNI in such a way that  
489 each switching node does not attach more than one site node. To  
490 realize a 1 + 1 protection scheme, a VN node needs to be mapped  
491 to two site nodes to form a primary-backup pair. If these two sites  
492 are connected to the same ingress/egress router, their network dis-  
493 tance would be 2 hops. We consider this an unsuitable scenario  
494 where the primary and backup sites can reside very close to each  
495 other and increase the possibility of both being affected during  
496 large-scale disasters. Therefore, we propose that the distance be-  
497 tween the primary and its backup site is at least 3 hops. Moreover,  
498 we limit the path length between the primary and backup site  
499 nodes by a threshold  $d_{th}$ , with a view to make sure that primary  
500 and backup sites are not too far away from each other. Hence,  
501 we have one more constraint for objective (3): For a candidate  
502 primary-backup pair of VN node  $i$ , we have,

$$3 \leq |p(i_p \rightarrow i_b)| \leq d_{th} \quad (13)$$

503 The primary-backup node distance constraint  $d_{th}$  is a network  
504 operational parameter which can be determined by a VNO. In or-  
505 der to geographically distribute primary and backup sites, a backup  
506 site node can also be considered even though the path length be-  
507 tween the primary-backup pair is longer than  $d_{th}$ . However, a large  
508 value of primary-backup pair path length may increase the com-  
509 munication cost for service backup to achieve site protection and  
510 network downtime during migration from primary to backup sites  
511 due to a longer network distance. It should be noted that  $d_{th}$  is  
512 not a compulsory constraint and our proposed VNE algorithm can  
513 work without it. However, we believe that (13) helps in keeping a  
514 primary-backup pairs at the right distance. In practice, a Telecom  
515 operator knows how its PNI is deployed and what could be the  
516 right distance between a primary-backup pair. The operator can  
517 then use (13) to reflect the desirable distance in the VNE process  
518 or can advertise to a VNF. We will perform detailed investigation  
519 on (13) in our future work. In this paper, we assume distance in  
520 routing hops.

521 Searching all the candidate primary-backup pairs for all the  
522 VN nodes takes up time and computing resources, and is also  
523 unnecessary especially for a large scale PNI. Greedy node map-  
524 ping algorithm is applied here for primary and backup site nodes  
525 mapping. For a VN node  $i$ , its capacity requirement is  $C_v(i)$  and  
526 its BW requirement is the summation of the BW required from  
527 all its incident links  $\sum_{j=1, j \neq i}^{|V_v|} B_v(i, j)$ . We first sort the VN nodes  
528 according to their required capacity in decreasing order as  $V_v =$   
529  $\{n_v^1, n_v^2, \dots, n_v^{|V_v|}\}$  and use this sequence to map the VN nodes to  
530 the site nodes in the PNI. The rationale behind this is that it is  
531 more difficult to embed a node with a high capacity requirement  
532 than a low capacity VN node. Site nodes with sufficient capacity  
533 are considered as candidates for VN node mapping and any two  
534 candidate site nodes form a candidate primary-backup pair. How-  
535 ever, searching the optimized primary-backup pair is complex in  
536 terms of computing resource and time. Geographical constraints  
537 could be added to assist site node selection as in [7], but they are  
538 not considered here due to space constraints. We simply limit the  
539 number of selected site nodes per each VN node by a fixed number  
540  $n_{nm}$  (e.g.  $n_{nm} = 5$ ). In the next step, the candidate pairs are sorted  
541 according to the hop count in an increasing order. If several pairs  
542 have the same hop count, the pair with higher capacity is put on  
543 top of the pair with lower capacity. We choose the first  $n_{th}$  pairs  
544 as the selected primary-backup pairs. If the number of candidate  
545 pairs is smaller than  $n_{th}$ , all the pairs are selected. For a VN node  $i$ ,  
546 it then has  $n_i$  candidate primary-backup pairs, where  $n_i \leq n_{th}$ . All  
547 the site nodes in the candidate primary-backup pairs is given by

$V_{pb}^i = \bigcup_{x=1}^{n_i} \{i_{p_x}, i_{b_x}\}$  where  $i_{p_x}$  and  $i_{b_x}$  represents the primary and  
548 backup nodes from the  $x$ th candidate pair respectively. Primary  
549 and backup nodes can be randomly decided within the primary-  
550 backup pairs or based on their capacity. For instance, a node with  
551 higher capacity is the primary node. We assume that each site  
552 node can only be mapped to one VN node within one VNE re-  
553 quest. Therefore, after establishing  $V_{pb}^i$ , all the nodes within  $V_{pb}^i$   
554 are reduced from the site nodes as  $V_r = V_r \cap (V_{pb}^i)^c$ , where  $(V_{pb}^i)^c$  is the  
555 absolute complement of  $V_{pb}^i$ .

## Algorithm 1

PBPS algorithm pseudo-code.

```

1:   procedure PBPS ( $G_p, G_v$ )
2:      $l_{ns} \leftarrow$  sort  $V_v$  (according to site capacity in decreasing order)
3:     for  $x \leftarrow 1, |V_v|$  do
4:        $l_{nm} \leftarrow \phi$ 
5:        $i' \leftarrow l_{ns}(x)$ 
6:       for all  $n_i^t \in V_r$  do
7:         if  $C_r(i) \geq C_v(i')$  then
8:            $l_{nm} \leftarrow l_{nm} \cup i'$ 
9:         end if
10:        if  $|l_{nm}| == n_{nm}$  then
11:          break
12:        end if
13:      end for
14:      if  $|l_{nm}| == 0$  then
15:        PBPS Fails
16:      end if
17:       $r \leftarrow 1, l_{pb}(x) = \phi$ 
18:      for  $i \leftarrow 1, |l_{nm}|, |l_{nm}|$  do
19:        for  $j \leftarrow i, |l_{nm}|$  do
20:          if  $|p(l_{nm}(i) \rightarrow l_{nm}(j))| \leq d_{th}$  then
21:             $l_{pb}(x) \leftarrow l_{pb}(x) \cup \{l_{nm}(i), l_{nm}(j)\}$ 
22:          end if
23:          if  $|l_{pb}(x)| == n_{th}$  then
24:            break
25:          end if
26:        end for
27:      end for
28:    end for
29:  end procedure

```

The searching of primary-backup pairs for the rest of VN nodes  
556 continues within the updated set of  $V_r$  until all the VN nodes  
557 form their own primary-backup pair sets. Primary-backup paths  
558 are found in this step as described above. By combining them with  
559 the primary-primary paths, we ensure a complete connectivity be-  
560 tween all nodes in two primary-backup pairs. The pseudo code of  
561 this Primary-Backup Pair Searching (PBPS) algorithm is shown in  
562 Algorithm 1.  
563  
564

## 4.2. VN link embedding

565 After selecting the primary-backup pairs for the VN nodes, the  
566 VN links between VN nodes are mapped to the paths on the PNI.  
567

(a) *Link embedding based on link degree:* VN links are mapped  
568 sequentially based on the node degree of the VN nodes. First, we  
569 sort the VN nodes according to their node degrees in the decreas-  
570 ing order  $V_v = \{n_v^1, n_v^2, \dots, n_v^i, \dots, n_v^{|V_v|}\}$ . The VN links are mapped  
571 from higher node degree VN nodes to lower node degree VN  
572 nodes. We assume that the node degree of VN node  $i$  is  $k$  and  
573 the node IDs of its neighbors are denoted as  $i^1, i^2, \dots, i^k$ . All the  
574 VN links that pass through the same VN node, e.g.  $e_v(i, i^x)$  for  
575  $\forall x \in [1, k]$ , have the same priority for mapping. In our algorithm,  
576 we sort  $i^x$  in increasing order and map  $e_v(i, i^x)$  using the sorted  
577 neighbor sequence. In the next step, the shortest paths between all  
578 the candidate pairs are established. Constraint-based Shortest Path  
579 First (CSPF) [23] can be used to determine the path with sufficient  
580 BW between all pairs. If the path length of a candidate pair cannot  
581

satisfy (13), this pair is removed from the candidate pair set. For a certain VN node, the BW constraint for its primary-backup pair is the summation BW of all links passing through this VN node.

This has two effects. Firstly, it correlates the node embedding with the link embedding. There is no point of selecting a node as the candidate which only has enough node capacity but not enough BW for ingress/egress links. Secondly, we only establish primary-primary paths in the PNI for inter VN node link embedding which is explained below.

(b) *Joint embedding of primary and backup paths*: Using the conventional 1 + 1 site protection approach as shown in Fig. 2 b, a mesh needs to be created among primary and backup nodes to ensure connectivity during any number of site failures. For example, for the VNE request of two connected nodes of A and B, in the conventional approach, we need to find out A and B, their respective backup nodes A' and B' and then interconnect all four of these. In our approach, we only connect the primary-backup pairs A–A' and B–B', and then we connect the primary nodes A–B, as shown in Fig. 2 c.

This way, we reuse a part of the primary-primary path to ensure connectivity among all 4 nodes if both A and B fail simultaneously or if one of them fails. The rationale behind this is, if the primary and backup sites are not too far away from each other (which would perform badly for backup data synchronization and migration-based switch over), the paths between two primary nodes and their backups would overlap for a large section. Therefore, to map two VN nodes, identifying three paths would suffice. If B fails, the path can be switched to B' from the intersection point of A–B and B–B'. Path searching between primary sites is a standard routing problem, which can be solved by many existing shortest path algorithms [23]. Constraint-based Shortest Path First (CSPF) is used in this work for route discovery in the PN, in which the required BW is the constraint. If the shortest path found in this way does not meet the delay requirement, we conclude that other paths will not either.

The conventional approach practically embeds the VNE request twice, and then connects the nodes in the primary network with nodes in the backup network in a mesh. Therefore, the number of paths ( $P_{con}$ ) for a VNE request  $G_V = (V_v, E_v)$  in worst case would be,  $P_{con} = 2E_v + \frac{2V_v(2V_v-1)}{2}$ .

Contrary to this, in our scheme, we only find out the paths requested in a VNE request and additionally, the paths between the primary-backup pairs. Therefore, the number of paths ( $P_{new}$ ) in our scheme would be,  $P_{new} = E_v + V_v$ , which is much smaller than  $P_{con}$  when  $V_v$  is large.

Please note that a primary path is interchangeable with its backup path in our scheme. For two given primary-backup pairs, the path with minimum length can be chosen to work as the primary path between these two pairs.

(c) *Embedded link adjustment*: After mapping the VN nodes, the VN link embedding process may not be successful in one trial. For instance, site nodes  $i$  and  $j$  are selected for VN node mapping, but there is no path that can be found between them after running CSPF because of BW scarcity. If this scenario occurs during the VN link embedding process, instead of using the BW constraint, we find out all paths between site nodes  $i$  and  $j$  that meet the delay constraint. We first take the shortest one and check if it overlaps with any previously embedded paths. If there are overlapping links, we check if releasing the previously embedded path would help releasing enough BW to embed the current path. If not, we go to the next shortest path between site nodes  $i$  and  $j$ , and do the same as above. If releasing the previously embedded path can help in embedding the current one, we release the previous one, embed the current VN link and re-embed the previous VN link as has been explained before. In order to avoid an algorithm loop, we mark all the overlapped links in the PNI. If further VN link embedding over-

**Table 2**  
Simulation parameters.

Parameter	Value
Physical node capacity	[100, 300]
Physical link bandwidth	[100, 200]
Node capacity in VNE request	[1, 5]
Link bandwidth in VNE request	[1, 5]
Number of nodes in VNE request	[2, 5]
Link delay limit in VNE request	10 hops
Primary-backup node distance	4 hops
Link probability in VNE request	0.5

laps on such marked links again, we exit the algorithm and declare a failure. This is because releasing a previously embedded path going through the marked links means that when re-embedding this released path, it will have the same overlapping link(s), releasing which will take us into a loop. If all the paths satisfying delay constraints do not overlap with any previously embedded paths, path searching fails, which means that there is no path available in the PNI to meet the BW requirement.

#### 4.3. Algorithm complexity discussion

The algorithm complexity should be considered separately for node selection and link selection. For node selection, let us suppose that there are  $m$  virtual nodes and  $n$  physical nodes, in which we assume that there are  $cn$  resource node and  $(1-c)n$  switching nodes. For each virtual node, we go through all possible resource nodes (with linear complexity  $O(n)$ ), and for each selected resource node, we run the shortest path search to find a backup (with complexity  $O(n^2)$ ). Therefore, the primary and backup site nodes searching for one virtual node has the complexity of  $O(n) + O(n^2)$ , which is  $O(n^2)$ . For  $m$  virtual nodes, we have complexity  $m \times O(n^2)$  which is  $O(n^2)$  when  $m$  is a constant number. For link selection, our proposed algorithm selects the shortest path between two primary nodes, therefore, it has the same complexity as the shortest path searching algorithm i.e.  $O(n^2)$ . Thus, the summation of the two parts is still  $O(n^2) + O(n^2)$ , which makes the complexity of our proposed VNE algorithm  $O(n^2)$  and thus, can be solved in polynomial time.

## 5. Performance evaluation

In this section, we provide the simulation-based evaluation results of our proposal against the conventional approach to achieve 1 + 1 site protection.

### 5.1. Simulation settings

(a) *Physical network*: To evaluate the performance of our algorithm, we have implemented a MATLAB based discrete event simulator. We randomly generate  $|V_s|$  switching nodes in a circular area to form the core transport network. Each switching node selects the five closest neighbors in terms of distance as its direct neighbors. We also generate  $|V_r|$  site nodes, which are randomly attached to one of the switching nodes. Any two site nodes cannot attach to the same switching node. The major simulation-related parameters are listed in Table 2. The capacity and bandwidth of each site node and switching node are uniformly distributed within the range [100, 300] and [100, 200] respectively. For capacity and bandwidth, we do not present any unit. For bandwidth, it could be K/M/Gbps. It could also be the numbers of  $\lambda$  in an optical network. For capacity, the unit could range from the number of physical machines, or VMs possible to accommodate to the numbers of CPU cores available. Network operators can decide in which granularity they want to perform capacity management.



**Table 3**

Comparison of best, conventional and our solution in terms of path length.

Number of switching nodes	13	16	18	22
Analytical model (best solution)	6.86	7.76	7.44	8.22
Conventional approach	9.3	9.7	10.06	10.78
New algorithm (our proposal)	9.3	9.7	10.06	10.78

696 (b) *VNE request*: For one VNE request, the number of requested  
 697 VN nodes is set to a fixed number 3, and the probability of connect-  
 698 tivity between every two VN nodes is 0.5. If all the nodes within  
 699 the VNO graph are not connected via single or multiple hops, the  
 700 VNO graph is regenerated. The bandwidth and capacity require-  
 701 ments are uniformly distributed within the range [1, 5]. The delay  
 702 limit for a VNE request is set to 10 hops. The path length limit  
 703 between a pair of primary and backup site nodes is 4 hops. The  
 704 number of selected primary and backup candidate pairs  $n_{th}$  is set  
 705 to 1.

## 706 5.2. Performance evaluation

707 In this section, we evaluate the performance of our proposed al-  
 708 gorithm to achieve 1 + 1 site protection. We simulate the arrival of  
 709 VNE requests as discrete events. To test the maximum number of  
 710 VNE requests that can be embedded in a PNI, we do not define the  
 711 lifetime of a VNE request. Hence, once a VNE request is embedded  
 712 in the PNI, it will remain in the network for the rest of the simu-  
 713 lation. For averaging, different number of iterations are performed  
 714 in different comparisons below. In general, 200 simulation runs are  
 715 used, unless specified otherwise, e.g. in (a) *Overall comparison* be-  
 716 low, we use 50 iterations as it is highly time-consuming to search  
 717 the whole problem space in order to find out the best solution.

718 (a) *Overall comparison*: To evaluate the performance of our pro-  
 719 posal, we use primary path length as an indicator which is the  
 720 summation of the hop counts from all the primary paths of a VNE  
 721 request. We compare the results averaged over 50 iterations for the  
 722 heuristic, with the optimal results derived from exhaustive search  
 723 over the whole problem space to find out all the primary-backup  
 724 possibilities in the analytical model. The analytical model is built  
 725 on the conventional approach, which requires full mesh between  
 726 all the primary and backup sites. In this study, the number of site  
 727 nodes is fixed to 10, and the number of switching nodes varies  
 728 between 13 and 22. Table 3 shows the results (*in terms of path*  
 729 *length*) obtained from different types of approach, where we com-  
 730 pare the embedded primary path lengths of the three types of ap-  
 731 proach. What should be noticed is that, to compare the bandwidth  
 732 consumption efficiency from different VNE solutions, we use the  
 733 same node mapping mechanism for primary-backup pair selection  
 734 in both conventional and our proposed algorithms to eliminate the  
 735 influence from the VN node embedding. This is also the reason  
 736 why the primary path lengths for these two algorithms (conven-  
 737 tional and our proposal) are the same as shown in Table 3. The  
 738 optimal solutions are obtained by searching the complete problem  
 739 space, and they therefore indicate the results that are not only op-  
 740 timized for node mapping but also for link mapping. The results  
 741 from the analytical model are superior to the heuristic algorithms,  
 742 but the required computing resources and computing time neces-  
 743 sary to achieve so cannot be neglected.

744 (b) *Bandwidth consumption*: As emphasized before, BW usage is  
 745 one of the main metrics to evaluate the VNE algorithm efficiency.  
 746 Therefore, we compare the BW consumption for each VNE request  
 747 by using both the conventional algorithm and our proposal. We  
 748 set up a PNI with 50 switching nodes and 20 site nodes. In order  
 749 to test the overall capability of the PNI to host the VNs, within  
 750 one simulation run, we input 20 VNE requests to one PNI sequen-

751 tially by using our proposal and the conventional approach. If one  
 752 VNE request can be embedded, its requested site node capacity  
 753 and link bandwidth are reserved for this VNE request. Otherwise  
 754 this VNE request is dropped. Fig. 3a depicts the BW consumption  
 755 for each VNE requests within one simulation run. A VNE request  
 756 that is generated earlier is associated with a smaller sequence ID  
 757 as shown in the X-axis in the figure. The Y-axis is the allocated  
 758 BW within the PNI for each VNE request with backup solution.  
 759 If a VNE request is rejected, the assigned BW is set to zero. The  
 760 results shown in the figure indicate that our proposed algorithm  
 761 consumes much less BW to embed a VNE request and it can also  
 762 accept more VNE requests than the conventional algorithm due to  
 763 its better resource allocation efficiency. To gain better understand-  
 764 ing about the algorithm performance, the simulation was repeated  
 765 200 times. For all the embedded VNE requests, the average BW  
 766 consumption for the embedded VNE request with the same se-  
 767 quence ID is shown in Fig. 3b, which indicates that the conven-  
 768 tional algorithm reserves around three times the BW compared to  
 769 our proposed algorithm. Moreover, the reserved BW while using  
 770 the conventional algorithm has a higher fluctuation than our pro-  
 771 posed algorithm.

772 (c) *Path length*: Based on the same simulation setup described  
 773 in the previous subsection, the total primary path length (paths  
 774 from primary site to primary site) and backup path length (paths  
 775 from backup site to backup site) has been investigated for each  
 776 VNE request. The results are shown in Fig. 4a. As shown in the  
 777 figure, for both conventional and our proposed algorithms, the pri-  
 778 mary path length is not always shorter than the backup length.  
 779 This is due to the fact that we setup the role of primary and  
 780 backup nodes (based on the site node capacities) before link em-  
 781 bedding. Therefore, the primary path length is not necessarily  
 782 shorter than the backup path. However, as mentioned before, pri-  
 783 mary sites can be selected based on the shorter path as well, as  
 784 primary and backup sites are interchangeable in our proposal. As  
 785 we can see, by using our proposed algorithm, the path length of  
 786 the backup path has a higher probability to be longer than the pri-  
 787 mary path. This phenomenon occurs because, after assigning the  
 788 primary backup pairs for a VNE request, we first select the short-  
 789 est path in the primary–primary site nodes which satisfies the BW  
 790 requirement. By doing so, the primary path is always the opti-  
 791 mized solution. Due to the fact that our proposed algorithm tries  
 792 to reuse part of the primary path to reduce the bandwidth reser-  
 793 vation for backup paths, the selection of backup paths might not  
 794 be optimized. This may result in longer backup path lengths than  
 795 the primary paths. In this work, we do not optimize the backup  
 796 path length. During a failure and the consequent site switchover,  
 797 the path to the backup PNI node could be optimized step by step.  
 798 In such cases, a new primary backup site pair will be formed, or  
 799 the failed primary site node can become the backup site node af-  
 800 ter its recovery and an unnecessary switchover back to it can be  
 801 avoided. We will address this in our future work. The average path  
 802 length for each embedded VNE request with the same sequence ID  
 803 is shown in Fig. 4b, which is based on 200 simulation runs. It also  
 804 indicates that the average backup path length of our proposed al-  
 805 gorithm is longer than the average primary path length, which is  
 806 not the case for the conventional algorithm.

807 (d) *VNE request acceptance ratio*: In order to gain better under-  
 808 standing about the above obtained results from Figs. 3b and 4b,  
 809 the VNE request acceptance ratio is plotted in Fig. 5, which is de-  
 810 fined as the ratio between the total number of accepted VNE re-  
 811 quests (successfully embedded) and the total number of simula-  
 812 tion iterations for this setup, which is the summation of success-  
 813 fully embedded and unsuccessfully embedded VNE requests. As  
 814 shown in the figure, it indicates that our proposed algorithm sees a  
 815 mild decrease in acceptance rate as the number of embedded VNs  
 816 increases in the network. In comparison, the decrease shown by

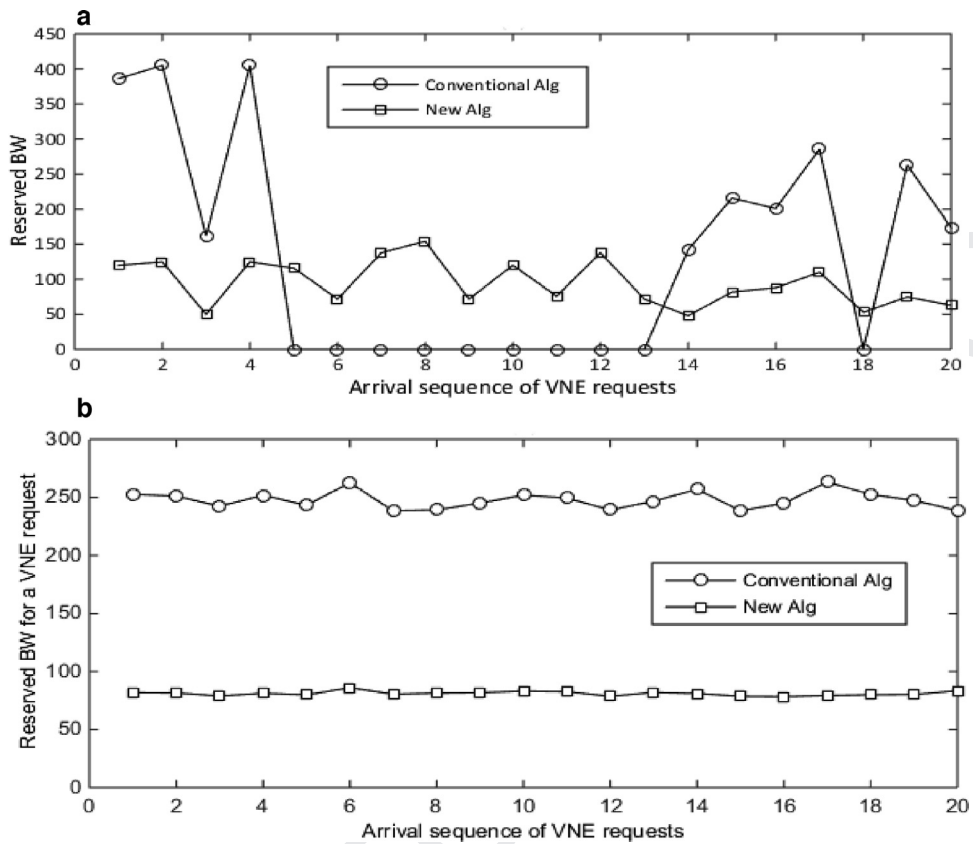


Fig. 3. Bandwidth consumption comparison between the conventional approach and our proposed algorithm.

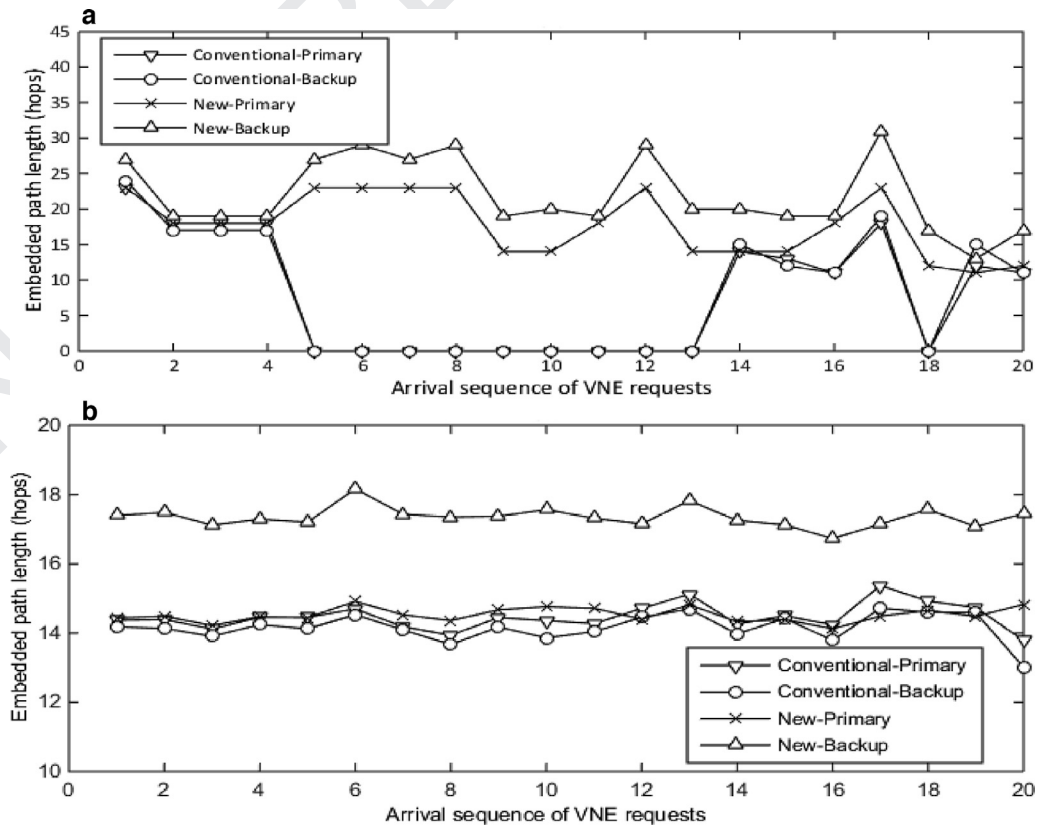


Fig. 4. Path length comparison between the conventional approach and our proposed algorithm.

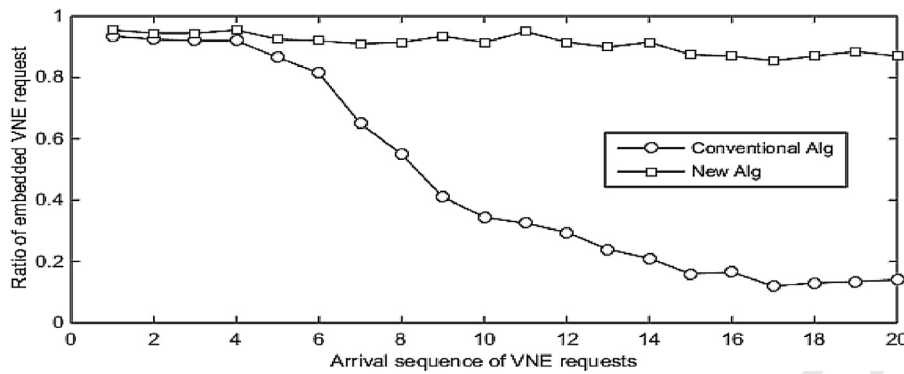


Fig. 5. VNE requests acceptance ratios for the conventional approach and our proposed algorithm.

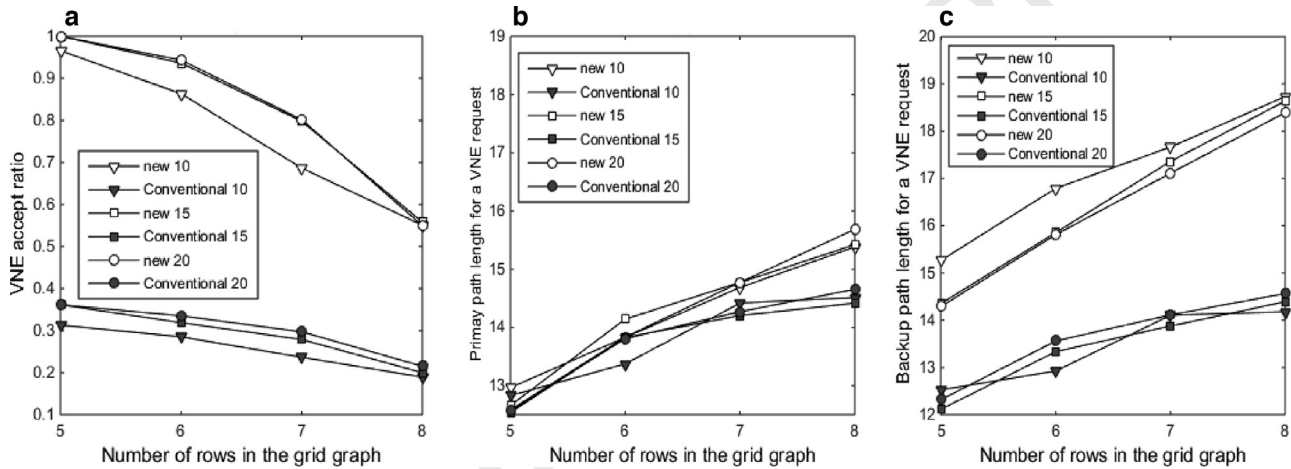


Fig. 6. Physical network scale influence on the embedding performance.

817 the conventional algorithm is more dramatic. This is because the  
818 more VNE requests are embedded in the PNI, the less resources  
819 are left to embed the later VNE requests (having higher sequence  
820 ID). In our scheme, we require much less resource than the con-  
821 ventional scheme, hence the VNE request acceptance ratio tends to  
822 be higher. In comparison, the conventional scheme fails to come  
823 up with an embedding solution when resources become scarce.

824 (e) *Physical network scale influence*: The size of a PNI also in-  
825 fluences the VNE performance. To investigate the PNI scale influ-  
826 ence, we generate a core transport network with a grid topol-  
827 ogy. The number of switching nodes is set to  $5 \times 5$ ,  $6 \times 6$ ,  $7 \times 7$   
828 and  $8 \times 8$  in different simulation scenarios. Moreover, the number  
829 of site nodes is varied from 10, to 15 to 20, and they are ran-  
830 domly attached to the switching nodes. The results shown in Fig.  
831 6 are the mean value after 100 iterations, in order to average the  
832 randomness effect. The number of VNE requests is set to 30 in  
833 each run of the simulation. We further compare the VNE request  
834 acceptance ratio under different scales of transport network and  
835 the results are shown in Fig. 6a. Our proposed algorithm has a  
836 much higher VNE request acceptance ratio than the conventional  
837 approach. When the network size increases, the acceptance ratios  
838 drop in both cases. There are two causes of VNE request drop.  
839 Once the core transport network becomes larger, the average dis-  
840 tance between site nodes also increases when the number of site  
841 nodes is fixed. Hence, the first cause of VNE request drop is the  
842 fact that the path length between the selected site nodes cannot  
843 satisfy the delay constraint specified by the simulation. This is a  
844 direct influence from the PNI topology. The second cause of VNE  
845 request drop lies in the BW within the PNI not being sufficient to  
846 host the VNE requests. When we further investigate the causes of

847 the VNE request drop by using these two algorithms, we find that  
848 the VNE request drop in our algorithm is mainly due to the first  
849 cause, and for the conventional one, it is mainly due to the second  
850 cause.

851 As shown in the figure, the results also indicate that the num-  
852 ber of site nodes also has certain impact on the acceptance ratio,  
853 i.e. the more site nodes we have, the better the acceptance ratio.  
854 More number of site nodes puts them closer to each other which  
855 helps in finding out paths requiring lower latency. Once the site  
856 node number becomes higher, the reason for embedding failure  
857 shifts to the scarcity of transport network resources.

858 In Fig. 6b and c, we show the average primary and backup path  
859 length for the embedded VNE requests in different PNI sizes. As  
860 shown in the figures, compared to the backup path length, the  
861 difference of primary path lengths between our proposed algo-  
862 rithm and the conventional algorithm is smaller. In our scheme,  
863 the primary path is the shortest path whereas in the conventional  
864 scheme, all paths are the shortest paths. Therefore, path lengths  
865 are similar for the primary paths in both schemes, whereas the  
866 backup path is longer in our scheme. In relation to this, it should  
867 be noted that our proposal has higher success rate (acceptance ra-  
868 tio) in larger PNI which also makes the path length longer while  
869 averaged over the total number of successful embedding.

870 Although our backup paths are few hops longer (Fig. 6c), we  
871 still consume fewer link resources (Fig. 4b). This is because we  
872 require to find and establish fewer links to ensure the necessary  
873 connectivity (Fig. 2b and c). Along with the reasons explained  
874 above for network scale, this is also the reason why we achieve  
875 higher acceptance ratio. As more and more VNE requests are  
876 embedded and consequently resources run out, the algorithm which

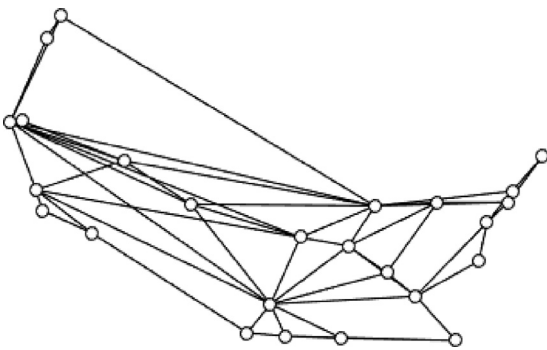


Fig. 7. US IP backbone topology.

## 6. Realization under NFV context

905

In this section, we explain the relevance of our work within the context of Network Functions Virtualization (NFV) as specified by European Telecommunications Standards Institute (ETSI) Industry Specification Group (ISG) NFV. ETSI ISG NFV has been formed by major operators and vendors to define global standard specifications for Telecom network virtualization. A virtualized implementation of a Network Function (e.g. mobile core nodes [2]) is called a Virtualized Network Function (VNF) which may contain multiple sub-components running in different VMs. These VMs could be located in the same datacenter i.e. site, or in multiple sites, according to the VNF deployment requirements and policies. In this paper, we have made the problem formulation such that a VNE request is embedded to geographically distributed sites connected by a Transport Network (TN). However, when a single VNF which is analogous to a VN node in our model, consists of multiple sub-components, the sub-components may need to be embedded within the same site. Besides, there could be a request to embed a chain of VNFs and each of the VNFs may contain multiple sub-functions as shown in Fig. 9. Whatever may be the scenario is, the VNE request can be formed as  $G_v = (V_v, E_v)$  as explained in Section 3.2. In such a case,  $V_v$  represents the sub-components of a VNF, and  $E_v$  represents the intra-VNF links connecting those sub-components.

Fig. 10 is the NFV reference architecture proposed by ETSI ISG NFV [24]. Functional blocks such as the Orchestrator, Virtualized Infrastructure Manager and VNFs as shown in Fig. 10 are the major relevant entities for VNF embedding. The embedding request is sent to NFV Orchestrator (NFVO), which will trigger the embedding decisions on the VNF Managers (VNFM). VNFMs manage the life-cycles of VNF instances. Virtualized Infrastructure Manager (VIM) controls and manages the compute, storage and network resources analogous to the PNI. A network within a site (e.g. datacenter) under the NFV context refers to the datacenter networks, which normally consist of different types of switches, e.g. core switches, aggregation switches and top of the rack switches, and all the switches are deployed according to certain pre-defined topology, e.g. two/three-tier tree, fat-tree, etc. If multiple sites are involved in deploying one VNF or a VNF chain, the TN (core transport network in Section 3) is also involved in the process. In this case, embedding needs to be done in two steps. Step 1 is the top-tier embedding, which selects suitable sites and links within the TN

consumes fewer resources achieves higher acceptance ratio i.e. is successful in the embedding when resources are scarce.

An implication of longer backup path is the usage of suboptimal paths after failure. Once a primary VN node is switched to its backup node, the path length to the backup node from other connected VN nodes will be suboptimal. These paths can slowly be optimized step by step once switching over to the backup node is completed without interfering with the intended service delivery.

(f) *Real network topology*: In order to understand our proposed algorithm performance in real networks, we use the data from topology zoo [25]. The used topology (Fig. 7) is from ATT North America with 25 switching nodes. We re-run the simulation with the same parameter setup as mentioned before (see Table 2). We show the Cumulative Distribution Function (cdf) of the embedded path length in Fig. 8a when the number of site nodes vary from 10, to 15, to 20.

In Fig. 8a, total path length of all successful VNE is plotted. Although our scheme has longer backup paths, it still performs better as it realizes a requested VN with less number of paths than the conventional approach. As illustrated by the results, the variation of site nodes (i.e. from 10 to 20) has influence on the embedded path length for a VNE request by using our scheme compared to the results obtained by using conventional scheme. Fig. 8b reconfirms a result from Fig. 6a, which shows that VNE acceptance ratio increases with the number of site nodes available. However, as seen in Fig. 6a, this increase becomes less prominent after a certain number of site nodes (15 site nodes in Fig. 8b). After this point, the VNE failures occur due to the scarcity of transport resources.

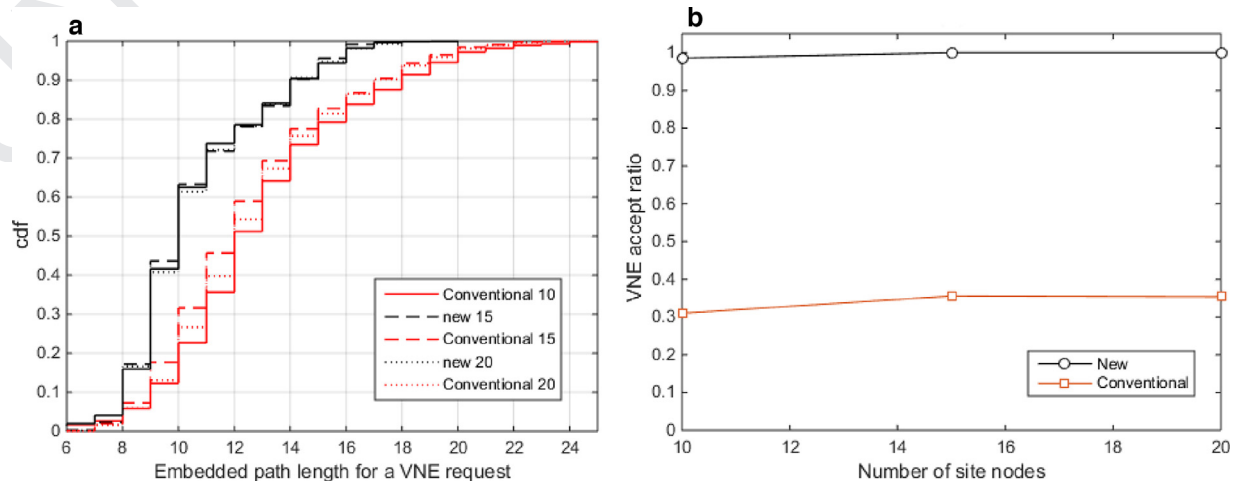


Fig. 8. Comparison of the conventional and our proposed algorithm in real network topology.

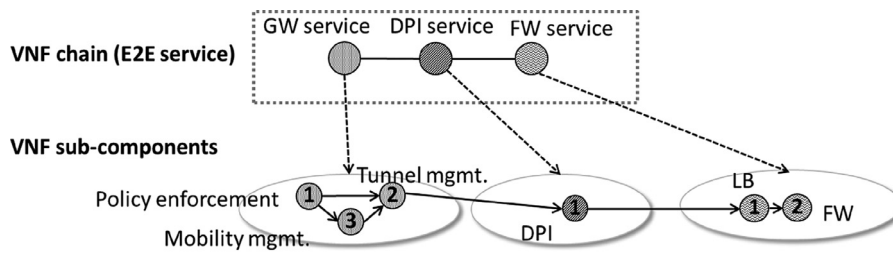


Fig. 9. VNF chain example.

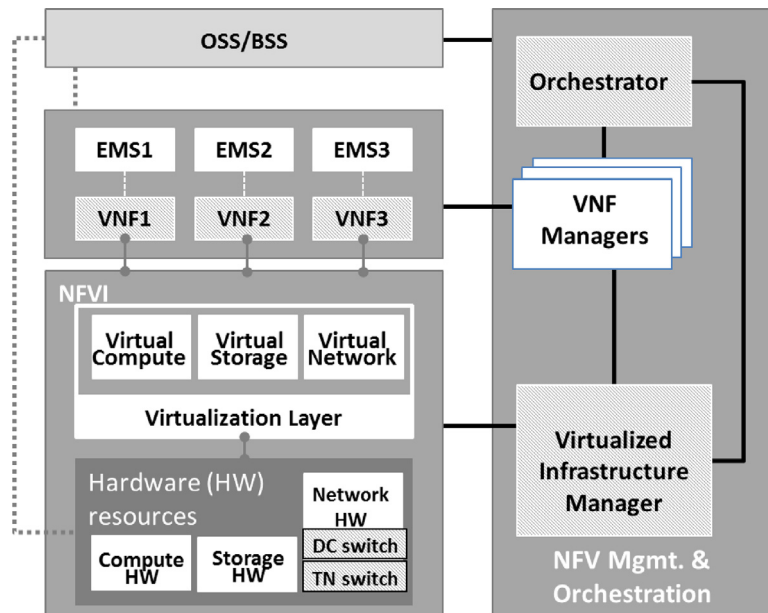


Fig. 10. NFV reference architectural framework.

947 that interconnect the sites. Step 2 is the local embedding: i.e. the  
 948 sub-components of each VNF need to be within a site where multiple  
 949 VMs are instantiated on different physical machines and connected  
 950 through intra-site links. Therefore, the infrastructure graph for  
 951 physical network  $G_p = (V_p, E_p)$  should be formulated and updated  
 952 accordingly by taking the switches of different types and capabilities  
 953 inside the site into consideration. If the TN is not involved, the  
 954 VNE algorithm can be run in VIM. If multiple VIMs and the TN  
 955 between are involved in the VNE process, the top tier VNE  
 956 will run in the Orchestrator and our proposed algorithm needs to  
 957 be deployed in both the VIM and the Orchestrator to ensure overall  
 958 protection.

## 959 7. Conclusions

960 In this paper, we have proposed and evaluated a heuristic algo-  
 961 rithm which realizes VNE for 1 + 1 site protection to meet Telco-  
 962 grade network protection and service availability requirements. In  
 963 approaching this issue, we do not relax the problem by using path  
 964 splitting as that is unrealistic in operational networks. We also dis-  
 965 tinguish between server nodes and switching nodes, as a server  
 966 node cannot be mapped on a switching node.

967 Our algorithm achieves sound correlation between node and  
 968 link embedding, consumes less bandwidth and provides higher  
 969 success rate than any conventional approach. Evaluation results  
 970 also show that our algorithm performance in finding out a VNE  
 971 solution is close to the theoretical ceiling. In our future work, we  
 972 will address VN node mapping over multiple sites in order to fur-  
 973 ther optimize site resources and backup path optimization in order

974 to further reduce the consumption of link resources. In addition,  
 975 we intend to further analyze the performance of the proposed VNE  
 976 algorithm in failure scenarios focusing of service recovery latency.

## References

- [1] W. Kellerer, J. Widmer, A. Khan, D. Jurca, Future mobile network: use cases for network virtualization, in: Proceedings of the 9th Wuerzburg Workshop on IP: Joint ITG and EuroNF Workshop Visions of Future Generation Networks (EuroView'09), July 2009, Germany, 2009.
- [2] 3GPP TS 23.401, General Packet Radio Service (GPRS) enhancements for Evolved Universal Terrestrial Radio Access Network (E-UTRAN) access, Technical Specification Group Services and System Aspects, 3rd Generation Partnership Project.
- [3] Y. Takano, A. Khan, M. Tamura, S. Iwashina, T. Shimizu, Virtualization-based scaling methods for stateful cellular network nodes using elastic core architecture, in: Proceedings of the 6th IEEE International Conference on Cloud Computing Technology and Science (CloudCom'14), December 2014, 2014.
- [4] T. Shimizu, T. Nakamura, Kiuchi M, A. Iwata, Y. Kubota, M. Ohhashi, An experimental evaluation of dynamic virtualized networking resource control on an evolved mobile core network, in: Proceedings of the Humanitarian Technology Conference (HTC'13), August 2013, IEEE, 2013.
- [5] A. Khan, W. Kellerer, K. Kozu, M. Yabusaki, Network sharing in the next mobile network: TCO reduction, management flexibility, and operational independence, IEEE Commun. Mag. 49 (10) (2011) 134–142.
- [6] S. Sharma, M. Chawla, A technical review for efficient virtual machine migration, in: Proceedings of the International Conference on Cloud & Ubiquitous Computing & Emerging Technologies (CUBE'13), November 2013, IEEE, India, 2013.
- [7] M. Chowdhury, M.R. Rahman, R. Boutaba, ViNEYard: virtual network embedding algorithms with coordinated node and link mapping, IEEE/ACM Trans. Netw. 20 (1) (2012) 206–219.
- [8] A. Khan, X. An, D.P. Caparros, W. Kiess, Virtual network embedding algorithm for one-to-one site protection, in: Proceedings of the IEEE Global Communications Conference (GLOBECOM'13), December 2013, Atlanta, GA, 2013.

- 1007 [9] T. Yamasaki, A. Khan, M. Tamura, T. Shimizu, S. Iwashina, A database access  
1008 scheme for elastic-core architecture, in: Proceedings of the IEEE APWiMob'14,  
1009 August 2014, Bali, Indonesia, 2014.
- 1010 [10] A. Jarray, A. Karmouch, Cost-efficient mapping for fault-tolerant virtual net-  
1011 works, *IEEE Trans. Comput.* 64 (3) (2015) 668–681.
- 1012 [11] Z. Qiang, W.H. Qiang, F.G. Sheng, L.H. Wu, Heuristic survivable virtual network  
1013 embedding based on node migration and link remapping, in: Proceedings of  
1014 the IEEE 7th Joint International Information Technology and Artificial Intelli-  
1015 gence Conference (ITAIC'14), December 2014, Chongqing, China, 2014, pp. 181–  
1016 185.
- 1017 [12] J.A. Johnson, Optimization of migration downtime of virtual machines in cloud,  
1018 in: Proceedings of the IEEE 4th International Conference on Computing, Com-  
1019 munications and Networking Technologies (ICCCNT'13), July 2013, India, 2013,  
1020 pp. 1–5.
- 1021 [13] Y. Chen, Ayoubi S, C. Assi, CORNER: Cost-Efficient and Reliability-Aware Virtual  
1022 Network Redesign and Embedding, in: Proceedings of the IEEE 3rd Interna-  
1023 tional Conference on Cloud Networking (CloudNet'14), October 2014, Luxem-  
1024 bourg, 2014, pp. 356–361.
- 1025 [14] M. Pourvali, H. Bai, F. Gu, K. Shaban, M. Naeini, J. Crichigno, M. Hayat, S. Khan,  
1026 N. Ghani, Virtual network mapping for cloud services under probabilistic re-  
1027 gional failures, in: Proceedings of the IEEE 3rd International Conference on  
1028 Cloud Networking (CloudNet'14), October 2014, Luxembourg, 2014, pp. 407–  
1029 412.
- 1030 [15] B. Guo, C. Qiao, J. Wang, H. Yu, Y. Zuo, J. Li, Z. Chen, Y. He, Survivable virtual  
1031 network design and embedding to survive a facility node failure, *IEEE J. Light-*  
1032 *wave Technol* 32 (3) (2014) 483–493.
- 1033 [16] A.N. Patel, Z. Ye, P.N. Ji, C. Qiao, Survivable virtual infrastructure mapping  
1034 with shared protection in transport software defined networks (T-SDNs), in:  
1035 Proceedings of the OptoElectronics and Communication Conference and Aus-  
1036 tralian Conference on Optical Fibre Technology (OECC/ACOFT '14), July 2014,  
1037 Melbourne, Australia, IEEE, 2014, pp. 679–681.
- [17] G. Liu, S. Su, Virtual network mapping algorithm with substrate node re- 1038  
liability awareness and shared-path protection, in: Proceedings of the IEEE 1039  
10th International Conference on High Performance Computing and Commu- 1040  
nications & Embedded and Ubiquitous Computing (HPCC\_EUC '13), November 1041  
2013, Zhangjiajie, China, 2013, pp. 636–643.
- [18] T. Guo, N. Wang, K. Moessner, R. Tafazolli, Shared backup network provision 1043  
for virtual network embedding, in: Proceedings of the IEEE International Con- 1044  
ference on Communications (ICC'11), June 2011, Japan, 2011.
- [19] M.R. Rahman, I. Aib, R. Boutaba, Survivable virtual network embedding, in: 1046  
Proceedings of the 9th International IFIP Networking Conference (NETWORK- 1047  
ING'10), May 2010, Chennai, India, Springer, Berlin, 2010, pp. 40–52. 1048
- [20] H. Yu, Migration based protection for virtual infrastructure survivability for 1049  
link failure, in: Proceedings of the Optical Fiber Communication Confer- 1050  
ence and Exposition and the National Fiber Optic Engineers Conference 1051  
(OFC/NFOEC'11), March 2011, Los Angeles, CA, IEEE, 2011. 1052
- [21] R.R. Oliveira, D.S. Marcon, L.R. Bays, M.C. Neves, L.P. Gaspar, M.P. Barcellos, 1053  
D. Medhi, Opportunistic resilience embedding (ORE): toward cost-efficient re- 1054  
silient virtual networks, *J. Comput. Netw.* (2015) (available online). 1055 Q6
- [22] S. Herker, X. An, W. Kiess, A. Kirstaedter, Path protection with explicit avail- 1056  
ability constraints for virtual network embedding, in: Proceedings of the IEEE 1057  
24th International Symposium on Personal, Indoor and Mobile Radio Commu- 1058  
nications (PIMRC'13), September 2013, London, UK, 2013, pp. 2978–2983. 1059
- [23] F. Kuipers, P. Van Mieghem, T. Korkmaz, M. Krunz, An overview of constraint- 1060  
based path selection algorithms for QoS routing, *IEEE Commun. Mag.* 40 (12) 1061  
(2002) 50–55. 1062
- [24] European Telecommunications Standards Institute (ETSI), "network functions 1063  
virtualization- introductory white paper", October 2012 [https://portal.etsi.org/](https://portal.etsi.org/nfv/nfv_white_paper.pdf) 1064  
[nfv/nfv\\_white\\_paper.pdf](https://portal.etsi.org/nfv/nfv_white_paper.pdf) . 1065 Q7
- [25] The University of Adelaide, The Internet Topology Zoo, [http://www.](http://www.topology-zoo.org) 1066  
[topology-zoo.org](http://www.topology-zoo.org). 1067